Organic Electronics

Deutsche Ausgabe: DOI: 10.1002/ange.201600113
Internationale Ausgabe: DOI: 10.1002/anie.201600113

Dibenzo[*a,j*]phenazine-Cored Donor–Acceptor–Donor Compounds as Green-to-Red/NIR Thermally Activated Delayed Fluorescence Organic Light Emitters

Przemyslaw Data, Piotr Pander, Masato Okazaki, Youhei Takeda,* Satoshi Minakata, and Andrew P. Monkman*

Abstract: *A new family of thermally activated delayed fluorescence (TADF) emitters based on U-shaped D-A-D architecture with a novel accepting unit has been developed. All investigated compounds have small singlet-triplet energy splitting (ΔE_{ST}) ranging from 0.02 to 0.20 eV and showed efficient TADF properties. The lowest triplet state of the acceptor unit plays the key role in the TADF mechanism. OLEDs fabricated with these TADF emitters achieved excellent efficiencies up to 16% external quantum efficiency (EQE).*

Over the last few decades, research on organic light-emitting diodes (OLEDs)[1] has greatly advanced. Indeed, many types of OLEDs can already be encountered in prototypical and commercial applications such as smartphones, lighting, and flat panel displays.[2] Currently, almost all the commercial OLEDs contain the rare metals such as Ir and Pt complexes because of their efficiency and stability.[3] Due to their high costs, the development of inexpensive and highly efficient emitters is desired. In OLEDs, the recombination of electrons and holes in an active material leads to the formation of various excited states such as singlet and triplet excitons, with the statistical probability of 25% and 75%, respectively.[4] With a conventional fluorescent emitter, the generated triplet excitons are dissipated through non-radiative (NR) processes. Therefore, to develop efficient OLEDs, these triplets should, in some way, be efficiently converted into emissive singlets, and to do so, without using a heavy metal atom-containing phosphorescent emitters, the phenomena of delayed fluorescence (DF), either via the process of triplet-triplet annihilation (TTA)[5] yielding a maximum 62.5% internal quantum efficiency,[6] or much better via thermally activated (or "E-type")[7] delayed fluorescence (TADF) attaining theoretically 100% harvesting of excitons,[8,9] can be used. To achieve efficient TADF, the energy difference between the excited singlet (S_1) and triplet state (T_1) ΔE_{ST} must be small (less than about 0.1 eV) so that the T_1 can efficiently backward transfer to the S_1 by thermal activation.[10] In this connection, twisted donor–acceptor (D-A) structures have been shown to be one of promising molecule scaffolds for TADF emitters,[8,9,11,12] because such structural motifs often allow effective HOMO/LUMO separation leading to small ΔE_{ST}. Nevertheless, many questions still remain about the TADF mechanism and molecular design principles. Furthermore, in contrast to the versatile options for D units, viable A units are quite limited.[13] Herein we disclose the development of a new family of efficient TADF emitters comprised of a new A unit core, dibenzo[*a,j*]phenazine (DBPHZ), and two Ds (Figure 1). Furthermore, these new emitters were found to yield green to deep-red/NIR OLED devices with high external quantum efficiencies (EQEs) up to 16%.

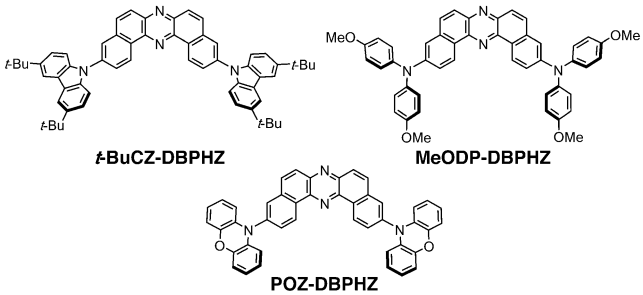

Figure 1. Structures of the investigated DBPHZs.

Recently, we have established a synthetic method to construct DBPHZ derivatives through an oxidative skeletal rearrangement of 1,1′-binaphthalene-2,2′-diamines (BINAMs).[14] With a slight modification of the original conditions, 3,11-dibromodibenzo[*a,j*]phenazine (**2**) was readily prepared from dibromo-substituted BINAM **1** in 50% yield (Scheme 1). The following Pd-catalyzed amination of **2** with the corresponding aromatic amines gave new family of D-A-D compounds that are otherwise difficult to synthesize (for the details, see the SI).

[*] Dr. P. Data, P. Pander, Prof. Dr. A. P. Monkman
Physics Department, Durham University
South Road, Durham DH1 3LE (UK)
E-mail: przemyslaw.data@durham.ac.uk
Dr. P. Data, P. Pander
Faculty of Chemistry, Silesian University of Technology
M. Strzody 9, 44-100 (Poland)
M. Okazaki, Prof. Dr. Y. Takeda, Prof. Dr. S. Minakata
Department of Applied Chemistry
Graduate School of Engineering
Osaka University, Yamadaoka 2-1, Suita
Osaka 565-0871 (Japan)
E-mail: takeda@chem.eng.osaka-u.ac.jp
Supporting information and the ORCID identification number(s) for the author(s) of this article can be found under http://dx.doi.org/10.1002/anie.201600113.

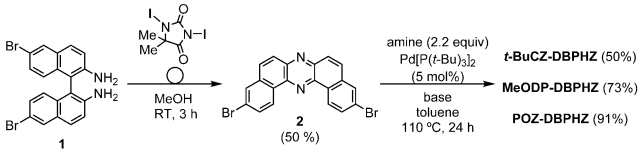

Scheme 1. Synthetic route to U-shaped D-A-D compounds.

A typical behavior of such fluorescent D-A compounds is to change their emission spectra as a function of the polarity of their environment. This is due to stabilization of the charge-separated character of their excited states over the locally excited character of D and/or A as polarity increases [Eq. (1)].

$$\Psi_{ICT} = c_1|D^*A>_{Loc} + c_2|DA^*>_{Loc} + c_3|D^+A^->_{CT} \quad (1)$$

Usually, emission in non-polar solvent comes from ^{1}LE (singlet locally excited state, $|D^*A>$ for example) which has $\pi\pi^*$ or $n\pi^*$ nature, and in more polar solvents the ^{1}CT (radical ion pair $|D^+A^->$) character dominates with emission shifted to lower energy through the polar stabilization process. Indeed, well resolved green to yellow emissions assignable to ^{1}LE were observed in their cyclohexane solutions (Figure 2). As reported recently,[9a] for compounds with weak to average ICT, that is, mixed character, ^{1}CT emission can be observed even in ethanol. However, with our new compounds ICT is strong, yielding excited states with dominant $|D^+A^->$ character, therefore emission in ethanol was not observed for all of them. Instead, the significantly red-shifted emissions derived from ^{1}CT were observed in THF for ***t*-BuCZ-DBPHZ** (orange, $\lambda_{em} = 537$ nm) and **MeODP-DBPHZ** (red, $\lambda_{em} = 613$ nm) (Figure 2). Notably, emission of

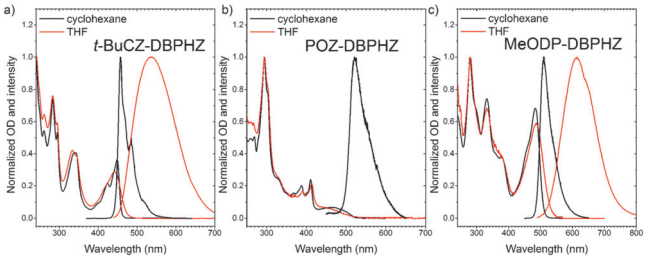

Figure 2. Absorption and PL spectra of a) ***t*-BuCZ-DBPHZ**, b) **POZ-DBPHZ**, and c) **MeODP-DBPHZ** solutions of specified solvent (concentration: 10^{-4} M).

POZ-DBPHZ was quenched even in degassed THF (Figure 2b), probably due to its stronger ICT character. With respect to absorption spectra, both of ***t*-BuCZ-** and **MeODP-DBPHZ** showed sharp absorptions in the lower energy region (400–500 nm) assignable to $\pi\pi^*$ transitions (Figure 2a,c). In contrast, **POZ-DBPHZ** exhibited a weak and broad peak in the similar energy region, but which was blue-shifted in a more polar solvent, indicating its $n\pi^*$ nature (Figure 2b).

Properties of DBPHZs are summarized in Table 1. Thermogravimetric analysis (TGA; see Figure S1 in the Supporting Information) of the D-A-D compounds revealed their high thermal stabilities [T_d (5 wt% loss) > 400 °C, Table 1], which is demanded for purification and fabrication of OLEDs by vacuum thermal deposition. Cyclic voltammetry (CV) showed reversible redox curves for all the compounds, indicating their promising electrochemical stability (Figure S2). The IP/EA values of DBPHZs determined by the CV experiments are indicated in Table 1.

Time resolved photoluminescence of 1 wt% DBPHZ derivative:zeonex blend films at 300 K revealed the presence of a delayed fluorescence (DF) component for all molecules (Figure S3). However, in the case of ***t*-BuCZ-DBPHZ**, the DF was very weak and phosphorescence (PH) dominated (Figure S3b). It was found that PH of ***t*-BuCZ-DBPHZ** originates from its acceptor unit (DBPHZ), as both PH spectra have similar structures (Figures S3a and S4). A small red shift in PH spectrum of ***t*-BuCZ-DBPHZ** (ca. 0.06 eV), compared to DBPHZ alone (Figure S4) in zeonex, is probably due to the change in electron density of the acceptor by the incorporation of the electron-donating carbazole units. For **MeODP-DBPHZ**, the T_1 is also lower in energy (2.21 eV) than the T_1 of the acceptor unit (2.40 eV), again attributed to the electron-donating influence of the donors on the DBPHZ core. Interestingly, the T_1 energy of **POZ-DBPHZ** is exactly the same as that of its azine core (2.40 eV). It may be concluded that the torsion angle between the DBPHZ core (A) and the phenoxazine (D) is very close to 90° such that Ds and A are electronically decoupled. This is significant as it has been shown that interconversion between ^{1}CT and ^{3}CT is forbidden via spin orbit coupling,[15] and ISC is mediated by a spin orbit charge transfer (SOCT) mechanism between ^{1}CT and a close lying local triplet state as is the reverse ISC process giving rise to TADF. To date, this phenomena has always been found with donor triplet (^{3}LE$_D$); it is noteworthy that this is the first unambiguously confirmed example of SOCT coupled with the acceptor triplet (^{3}LE$_A$). Thus in this molecule any TADF must be mediated by SOCT ^{1}CT-^{3}LE$_A$

Table 1: Summary of properties of DBPHZs.

Compd	λ_{abs} [nm] (in *c*-hex)[a]	λ_{em} [nm] (in *c*-hex[a]/ in CBP film[b])	Φ_{PL} (in *c*-hex[a]/ in CBP film[b])	IP/EA [eV][c]	E_s/E_T [eV] (in zeonex)[d]	ΔE_{ST} [eV] (in zeonex)	E_s/E_T [eV] (in CBP)[b]	ΔE_{ST} [eV] (in CBP)	T_d [°C][e]
***t*-BuCZ-DBPHZ**	449	457/509	0.61/0.31	−5.79/−3.37	2.77/2.34	0.43	2.67/2.34	0.33	472
POZ-DBPHZ	463	521/595	0.33/0.79	−5.36/−3.38	2.48/2.40	0.08	2.28/2.26	0.02	453
MeODP-DBPHZ	486	509/592	0.49/0.58	−5.30/−3.20	2.52/2.21	0.31	2.32/2.13	0.19	435

[a] Measured using cyclohexane solutions (10^{-5} M). [b] Measured using the 10 wt% DBPHZs:CBP films. [c] Estimated from the onset potentials ($^{ox}E_{onset}$ and $^{red}E_{onset}$ [eV] against Fc/Fc$^+$ redox couple) in CV experiments by the following equation: IP = −(5.1 + $^{ox}E_{onset}$) [eV]; EA = −(5.1 + $^{red}E_{onset}$) [eV]. [d] Measured using the 1 wt% DBPHZs:zeonex films. [e] The temperatures of 5 wt% loss.

coupling. A gradually decreasing ΔE_{ST} was observed with increasing electron-donating character of the donor: 0.43 eV for ***t*-BuCZ-DBPHZ**, 0.31 eV for **MeODP-DBPHZ**, and 0.08 eV for **POZ-DBPHZ**, which is consistent with increasing ICT character in the same order (Figure S3), suggesting that **POZ-DBPHZ** is an excellent candidate as a TADF emitter. DF activation energies (E_a) in zeonex estimated from Arrhenius plots (Figure S5) followed the same order as ΔE_{ST}: 0.26 eV for ***t*-BuCZ-DBPHZ**, 0.22 eV for **MeODP-DBPHZ**, and 0.05 eV for **POZ-DBPHZ**.

At 300 K both prompt and delayed emission arise from a ^{1}CT state (Figure S3), whereas at 80 K, prompt ^{1}CT and long lived phosphorescence (^{3}LE$_A$) were observed, indicative of a $\Delta E_{ST} \gg k_B T$. Focusing on **POZ-DBPHZ**, the DF gradually evolved with time (Figure S3d). The emission spectrum has a low-energy shoulder that decayed within a few milliseconds, followed by the growth of a high-energy shoulder in the millisecond regime (Figure S6a). This could be evidence for some structural changes occurring very slowly within the polymer matrix that increase the $c_2|DA^*>_{Loc}$ contribution of the excited state, or indicate that different molecular geometries exist within the films having different average decay times. The PH observed at 80 K also clearly showed the evolution of the spectrum with a monotonic increase of intensity in the 0-1 vibronic transition (Figure S6c), indicating a gradual change in the geometry into a more twisted configuration.

It was clearly seen that the lowering of ΔE_{ST} by 0.2 eV (0.31 eV for **MeODP-DBPHZ**, 0.08 eV for **POZ-DBPHZ**) decreased the DF lifetime by three orders of magnitude but increased the intensity by two orders (Figure S3). The lifetimes of the prompt fluorescence (PF) followed the opposite trend, indicative of an increased decoupling of the D and A fragments due to increased orthogonality between them.

Multiexponential fits were found for both prompt and delayed emission components (Figure S3b, d, and f). This again reflects the evolution of the emission spectra with time, and it would indicate the potential presence of different molecular geometries, which should be affected by any heterogeneous nature of the films and the environment around each molecule. Because zeonex is non polar, there is no environmental (polar) stabilization of the CT state and the absolute degree of CT within a molecule would be ill-defined, as described by Equation (1).

Dynamic photophysics of the compounds doped (10 wt%) in a small molecular host matrix CBP, which was then be used in subsequent OLED fabrication, was investigated (Figure 3). ***t*-BuCZ-DBPHZ** still exhibited weak DF. Its ^{1}CT red shifted from 2.77 eV in zeonex (Figure S3a) to 2.67 eV (Figure 3a), whilst its T_1 energy remained at 2.34 eV. For **MeODP-DBPHZ**, when compared to the films in zeonex, both S_1 and T_1 decreased in energy (ΔE_S 0.20 eV, ΔE_T 0.08 eV) in CBP matrix, and the PH appeared to be dominated by the 0-0 vibronic transition, indicative of the more rigid nature of the CBP matrix. We assumed that this phenomenon is caused due to packing effects and the increased polarity of CBP, which help to rigidify the **MeODP-DBPHZ** molecules in the host matrix. The increase of the DF contribution in the **MeODP-DBPHZ**:CBP blended

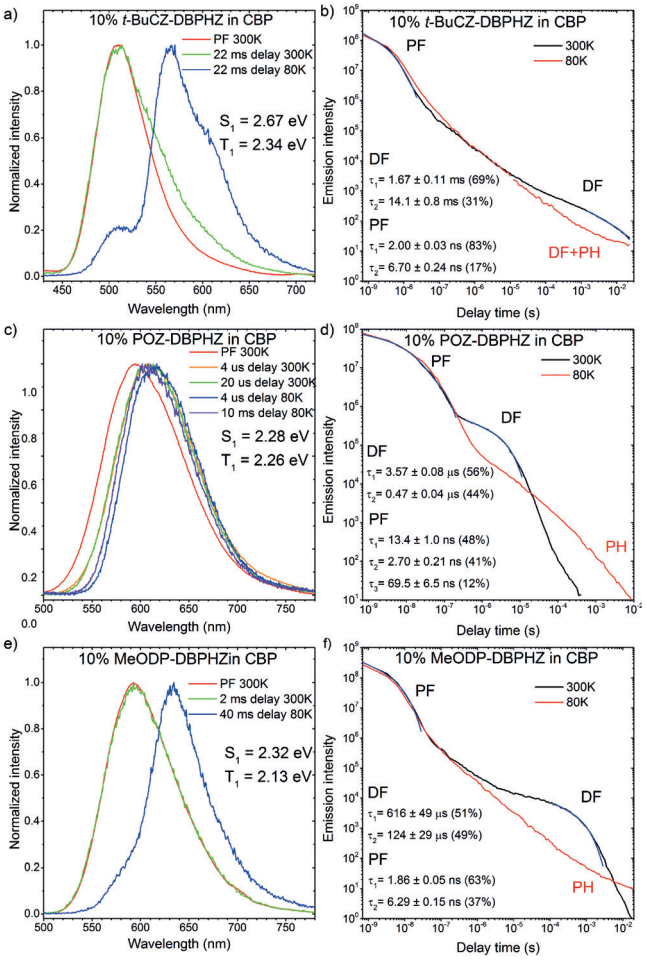

Figure 3. PF, DF, and PH spectra of 10 wt% a) ***t*-BuCZ-DBPHZ**, c) **POZ-DBPHZ**, and e) **MeODP-DBPHZ** in CBP blended films. Transient decays of 10 wt% b) ***t*-BuCZ-DBPHZ**, d) **POZ-DBPHZ**, and f) **MeODP-DBPHZ** in CBP films measured at 300 K and 80 K.

film was noticeable (Figure 3f) by some two orders of magnitude, compared to in zeonex (Figure S3f). Turning to **POZ-DBPHZ**, the situation was rather simple. Prompt and delayed ^{1}CT emissions were always observed, while no PH was detected (Figure 3c). The CT emission was red shifted in accord with the polar nature of the host, where the $c_3|D^+A^->_{CT}$ character of the excited state is dominant. Again, the spectral position moved in time, but now showing a monotonic red shift (Figure S7). Given the more rigid nature of the CBP host, this result would indicate the dispersion of ^{1}CT energies as a result of the inhomogeneity of the films: the more blue states with slightly more $c_2|DA^*>_{Loc}$ character decayed first and the more charge separated red states decayed with the longest lifetime, and thereby the spectrum effectively red shifted in time. As the temperature was lowered, the total emission of the **POZ-DBPHZ**:zeonex film fell off (Figure S5c), but an increase in the relative intensity of the blue edge emission (centered at around 540 nm) to the red edge emission was observed. This would suggest that as NR processes are suppressed, as the temperature lowered, it is the states with greater CT character that suffered more NR decay, as would be expected for the

longest-lived states in zeonex (Figure S6). In stark contrast, 10 ms after the excitation at 80 K, we observed a small blue shifted emission (by 0.02 eV) from **POZ-DBPHZ**:CBP film (Figure S7), suggestive of remnant PH from the ^3LE_A. This would indicate that the ^1CT state was stabilized below the ^3LE_A state by the CBP host but that they are now virtually isoenergetic. ***t*-BuCZ-DBPHZ** and **MeODP-DBPHZ** in CBP blends have very similar PF decay times (Figures 3b,f, S8, and S9), which may indicate that decoupling of the D and A units is only effective at torsion angles approaching 90°.

Given the near perfect linear power dependence in the analysis of the delayed emission intensity versus laser pulse fluence of the DBPHZ derivatives doped (1 wt%) in zeonex (Figure S10), TADF undoubtedly dominates in both **MeODP-DBPHZ** and **POZ-DBPHZ**, whereas for ***t*-BuCZ-DBPHZ**, triplet-triplet annihilation (TTA) (or mixed TTA TADF) cannot be excluded (Figures S3b and S10a). This measurement for ***t*-BuCZ-DBPHZ** could not be performed at 300 K due to the very weak DF/PH ratio at this temperature. Investigation of 10 wt% DBPHZ-doped films of CBP (Figure S10) showed similar behavior, and for ***t*-BuCZ-DBPHZ**, TTA still seems to be present.

The temperature dependence of the DF measured in zeonex films for ***t*-BuCZ-DBPHZ** and **MeODP-DBPHZ** was typical activated behavior (Figure S5),[9] while for **POZ-DBPHZ**, the maximum was observed at about 200 K (Figure S5d), indicating a NR relaxation starts to be significant above 200 K in **POZ-DBPHZ**. The E_a of 0.047 ± 0.002 eV was extracted from this plot. However, when the temperature dependence was investigated for 10 wt% **POZ-DBPHZ**:CBP blended film (Figure 4), no such quenching up to 300 K was

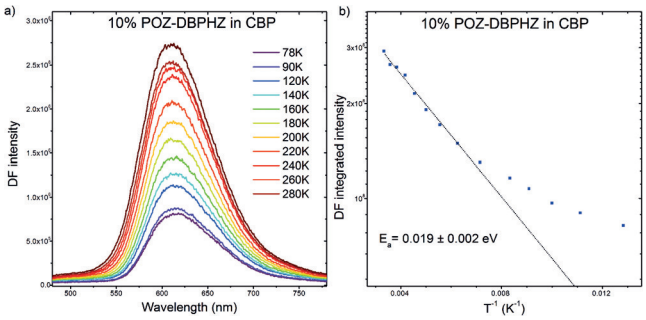

Figure 4. Temperature dependence of DF in 10 wt% **POZ-DBPHZ**:CBP blended film: a) spectra and b) plot of DF integrated intensity versus temperature with calculated activation energy.

observed, further supporting the idea that CBP packing helps to rigidify the TADF molecules thus preventing NR relaxation. Furthermore, the E_a of the DF emission was found to be 19 ± 2 meV (Figure 4b), indicating the relative shift of the ^1CT with respect to the ^3LE_A to reduce the activation barrier, which is a value comparable with that of the best exciplex ever.[16] The E_a for ***t*-BuCZ-DBPHZ** and **MeODP-DBPHZ** were found to be 0.026 eV and 0.024 eV, respectively (Figure S11). However, on close inspection of the temperature dependent spectra (Figure S11), it was seen that the ^1CT emission blue shifted and became structured, that is, ^1LE at around 130 K. We believe that the measured E_a relates to this process (freezing out of a critical vibrational mode) and not the E_a for TADF. The laser power dependence of DF in CBP was perfectly linear, indicative of activated reverse intersystem crossing (Figure S10).

To determine the efficiency of the TADF in these materials for harvesting triplets, OLED devices (DEV 1–3) were fabricated (Figure 5). The device structure used was as follows: ITO/NPB (40 nm)/10 wt% DBPHZ derivative in

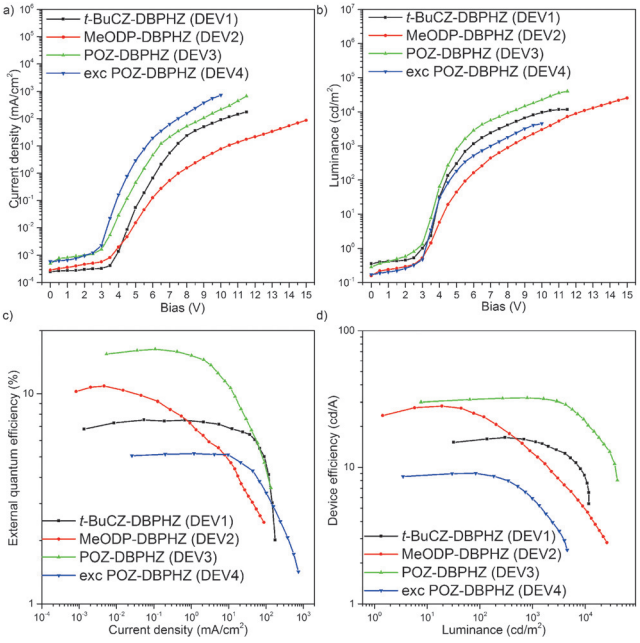

Figure 5. Device characteristic of DEV 1–4.

CBP (20 nm)/TPBi (20 nm)/BCP (20 nm)/LiF (1 nm)/Al (100 nm). The performance characteristics of the donor-host OLED structures (DEV1-3) revealed that high efficiencies (the maximum EQE about 16%) were obtained only for the **POZ-DBPHZ**-based device (DEV3, Figure 5c). For the ***t*-BuCZ-DBPHZ** and **MeODP-DBPHZ**, the efficiencies were about half this, which could be explained by two factors: 1) higher ΔE_{ST} compared to **POZ-DBPHZ**; 2) the much longer lived DF emission in these materials leading to potentially high charge quenching of the excited states. In the carbazole derivative, there is also a possible TTA contribution that could also diminish the overall efficiency. The luminance of device based on **POZ-DBPHZ** (DEV 3) was also twice as high (more than 35000 cd m^{-2}) as those for other compounds (Figure 5b).

The turn-on voltage was similar for all of devices around 3.7 V (Figure 5a). The OLED characteristic showed typical roll-off dependency, especially for **MeODP-DBPHZ**, and the highest observed EQE for this compound (10.3%, 10 cd m^{-2} luminance) fell off rapidly to be 9.1% at 100 cd m^{-2} and 6.3% at 1000 cd m^{-2} brightness. The luminous power efficiency and current efficiency at low luminance at 100 cd m^{-2} (19.2 lm W^{-1}, 31.2 cd A^{-1}) and high luminance at 1000 cd m^{-2} (12.4 lm W^{-1}, 30.5 cd A^{-1}) for **POZ-DBPHZ** indicate this is

a good TADF emitter for OLEDs and that the ^{1}CT coupling with ^3LE_A is promising for an efficient triplet harvesting as well as donor triplet coupled systems. For the purpose of tailoring emission colors and efficiencies, other host materials were tested with **POZ-DBPHZ** (Figures S12 and S13). Among them, *m*-MTDATA was found to form an exciplex[16] to show deep-red/near-infrared (NIR) emission (λ_{em} = 741 nm), and exciplex-based device formed with **POZ-DBPHZ** and *m*-MTDATA (DEV4, Figures 5 and S14) exhibited an EQE of about 5%, which is an excellent value for a TADF deep-red/NIR OLED.[17] The overall performances were much smaller than those of CT-based TADF devices, but exciplex emitters would give more opportunities for tailoring.

In summary, we have found that all members of this new family of D-A-D compounds based on a new acceptor core DBPHZ have TADF properties. The highest efficiency (up to 16%) was observed for the **POZ-DBPHZ** that bears very small E_a (ca. 19 meV) and ΔE_{ST}, and its orange emission would give us the excellent possibility for practical applications, such as two-color white OLEDs.[18] As expected for a thermally activated process, the magnitude of ΔE_{ST} has a great influence on OLED efficiency. Most importantly, the acceptor unit has the lowest ^{3}LE of the molecule, which couples to the donor ^{1}CT to provide the SOCT and hence spin-flip for efficient triplet harvesting. Notably, in the case of **POZ-DBPHZ**, this is the first unambiguously confirmed case where the triplet state coupling of acceptor produces efficient TADF, indicating that the generation of TADF is independent of which triplet state (D or A) couples to ^{1}CT. This finding greatly relaxes the design criterion for efficient TADF molecules. Furthermore, the important role of the emitter host has been observed in the **POZ-DBPHZ** systems. CBP performs two important roles: 1) as a polar environment that shifts the ^{1}CT level relative to the acceptor triplet to significantly reduce ΔE_{ST} to a value less than k_BT; 2) as a very rigid environment that reduces inhomogeneity and prevents NR decays to yield very efficient emission and devices.

Acknowledgements

This work was supported by the Polish Ministry of Science and Higher Education Mobility Plus project number 932/MOB/2012, and Open Partnership Joint Projects of JSPS (Japan Society for the Promotion of Science) Bilateral Joint Research Projects. The research leading to these results has received funding from the H2020-MSCA-IF-2014/659288 project "TADFORCE".

Keywords: charge transfer · electroluminescence · exciplexes · fluorescence · organic light-emitting diodes

How to cite: *Angew. Chem. Int. Ed.* **2016**, *55*, 5739–5744
Angew. Chem. **2016**, *128*, 5833–5838

[1] C. W. Tang, S. A. Van Slyke, *Appl. Phys. Lett.* **1987**, *51*, 913–915.
[2] a) S. R. Forrest, *Nature* **2004**, *428*, 911–918; b) *Organic Light Emitting Devices, Synthesis Properties and Applications*, (Eds.: K. Müllen, U. Scherf), Wiley-VCH, Weinheim, **2006**; c) *OLED Fundamentals, Materials, Devices and Processing of Organic Light-Emitting Diodes*, (Eds.: D. J. Gaspar, E. Polikarpov), CRC Press, Boca Raton, FL, **2015**.
[3] *Highly Efficient OLEDs with Phosphorescent Materials*, (Ed.: H. Yersin), Wiley-VCH, Weinheim, **2008**.
[4] a) A. R. Brown, K. Pichler, N. C. Greenham, D. D. C. Bradley, R. H. Friend, A. B. Holmes, *Chem. Phys. Lett.* **1993**, *210*, 61–66; b) M. A. Baldo, D. F. O'Brien, M. E. Thompson, S. R. Forrest, *Phys. Rev. B* **1999**, *60*, 14422–14428.
[5] J. Partee, E. L. Frankevich, B. Uhlhorn, J. Shinar, Y. Ding, T. J. Barton, *Phys. Rev. Lett.* **1999**, *82*, 3673–3676.
[6] a) S. Sinha, A. P. Monkman, *Appl. Phys. Lett.* **2003**, *82*, 4651–4653; b) C.-J. Chiang, A. Kimyonok, M. K. Etherington, G. C. Griffiths, V. Jankus, F. Turksoy, A. P. Monkman, *Adv. Funct. Mater.* **2013**, *23*, 739–746.
[7] C. A. Parker, C. G. Hatchard, *Trans. Faraday Soc.* **1961**, *57*, 1894.
[8] H. Uoyama, K. Goushi, K. Shizu, H. Nomura, C. Adachi, *Nature* **2012**, *492*, 234–238.
[9] a) F. B. Dias, K. N. Bourdakos, V. Jankus, K. C. Moss, K. T. Kamtekar, V. Bhalla, J. Santos, M. R. Bryce, A. P. Monkman, *Adv. Mater.* **2013**, *25*, 3707–3714; b) V. Jankus, P. Data, D. Graves, C. McGuinness, J. Santos, M. R. Bryce, F. B. Dias, A. P. Monkman, *Adv. Funct. Mater.* **2014**, *24*, 6178–6186.
[10] A. Endo, M. Ogasawara, A. Takahashi, D. Yokoyama, Y. Kato, C. Adachi, *Adv. Mater.* **2009**, *21*, 4802–4806.
[11] a) A. Endo, K. Sato, K. Yoshimura, T. Kai, A. Kawada, H. Miyazaki, C. Adachi, *Appl. Phys. Lett.* **2011**, *98*, 083302; b) G. Méhes, H. Nomura, Q. Zhang, T. Nakagawa, C. Adachi, *Angew. Chem. Int. Ed.* **2012**, *51*, 11311–11315; *Angew. Chem.* **2012**, *124*, 11473–11477; c) Q. Zhang, J. Li, K. Shizu, S. Huang, S. Hirata, H. Miyazaki, C. Adachi, *J. Am. Chem. Soc.* **2012**, *134*, 14706–14709; d) J. Li, T. Nakagawa, J. MacDonald, Q. Zhang, H. Nomura, H. Miyazaki, C. Adachi, *Adv. Mater.* **2013**, *25*, 3319–3323; e) J. Lee, K. Shizu, H. Tanaka, H. Nomura, T. Yasuda, C. Adachi, *J. Mater. Chem. C* **2013**, *1*, 4599–4604; f) S. Y. Lee, T. Yasuda, Y. S. Yang, Q. Zhang, C. Adachi, *Angew. Chem. Int. Ed.* **2014**, *53*, 6402–6406; *Angew. Chem.* **2014**, *126*, 6520–6524; g) T. Takahashi, K. Shizu, T. Yasuda, K. Togashi, C. Adachi, *Sci. Technol. Adv. Mater.* **2014**, *15*, 034202; h) S. Y. Lee, T. Yasuda, I. S. Park, C. Adachi, *Dalton Trans.* **2015**, *44*, 8356–8359; i) H. Kaji, H. Suzuki, T. Fukushima, K. Shizu, K. Suzuki, S. Kubo, T. Komino, H. Oiwa, F. Suzuki, A. Wakamiya, Y. Murata, C. Adachi, *Nat. Commun.* **2015**, *6*, 8476; j) K. Suzuki, S. Kubo, K. Shizu, T. Fukushima, A. Wakamiya, Y. Murata, C. Adachi, H. Kaji, *Angew. Chem. Int. Ed.* **2015**, *54*, 15231–15235; *Angew. Chem.* **2015**, *127*, 15446–15450.
[12] a) Y. J. Cho, S. K. Jeon, B. D. Chin, E. Yu, J. Y. Lee, *Angew. Chem. Int. Ed.* **2015**, *54*, 5201–5204; *Angew. Chem.* **2015**, *127*, 5290–5293; b) K. Albrecht, K. Matsuoka, K. Fujita, K. Yamamoto, *Angew. Chem. Int. Ed.* **2015**, *54*, 5677–5682; *Angew. Chem.* **2015**, *127*, 5769–5774; c) K. Kawasumi, T. Wu, T. Zhu, H. S. Chae, T. V. Voorhis, M. A. Baldo, T. M. Swager, *J. Am. Chem. Soc.* **2015**, *137*, 11908–11911.
[13] Y. Tao, K. Yuan, T. Chen, P. Xu, H. Li, R. Chen, C. Zheng, L. Zhang, W. Huang, *Adv. Mater.* **2014**, *26*, 7931–7958, and references therein.
[14] Y. Takeda, M. Okazaki, S. Minakata, *Chem. Commun.* **2014**, *50*, 10291–10294.
[15] B. T. Lim, S. Okajima, A. K. Chandra, E. C. Lim, *Chem. Phys. Lett.* **1981**, *79*, 22–27.
[16] a) K. Goushi, K. Yoshida, K. Sato, C. Adachi, *Nat. Photonics* **2012**, *6*, 253–258; b) D. Graves, V. Jankus, F. B. Dias, A. Monkman, *Adv. Funct. Mater.* **2014**, *24*, 2343–2351.

[17] a) H. Tanaka, K. Shizu, H. Nakanotani, C. Adachi, *Chem. Mater.* **2013**, *25*, 3766 – 3771; b) J. Li, T. Nakagawa, J. MacDonald, Q. Zhang, H. Nomura, H. Miyazaki, C. Adachi, *Adv. Mater.* **2013**, *25*, 3319 – 3323; c) Q. Zhang, H. Kuwabara, W. J., Jr. Potscavage, S. Huang, Y. Hatae, T. Shibata, C. Adachi, *J. Am. Chem. Soc.* **2014**, *136*, 18070 – 18081; d) S. Wang, X. Yan, Z. Cheng, H. Zhang, Y. Liu, Y. Wang, *Angew. Chem. Int. Ed.* **2015**, *54*, 13068 – 13072; *Angew. Chem.* **2015**, *127*, 13260 – 13264.

[18] H. A. Al Attar, A. P. Monkman, M. Tavasli, S. Bettington, M. R. Bryce, *Appl. Phys. Lett.* **2005**, *86*, 121101.

Received: January 5, 2016
Revised: February 16, 2016
Published online: April 6, 2016

